Average features of the interplanetary shock observed with the Global Muon Detector Network

M. Kozai[a], K. Munakata[a] , C. Kato[a] , T. Kuwabara[b] ,

M. Rockenbach[c], A. Dal Lago[d], N. J. Schuch[c], H. K. Al Jassar[e],

M. M. Sharma[e], M. L. Duldig[f], J. E. Humble[f], J. W. Bieber[g],

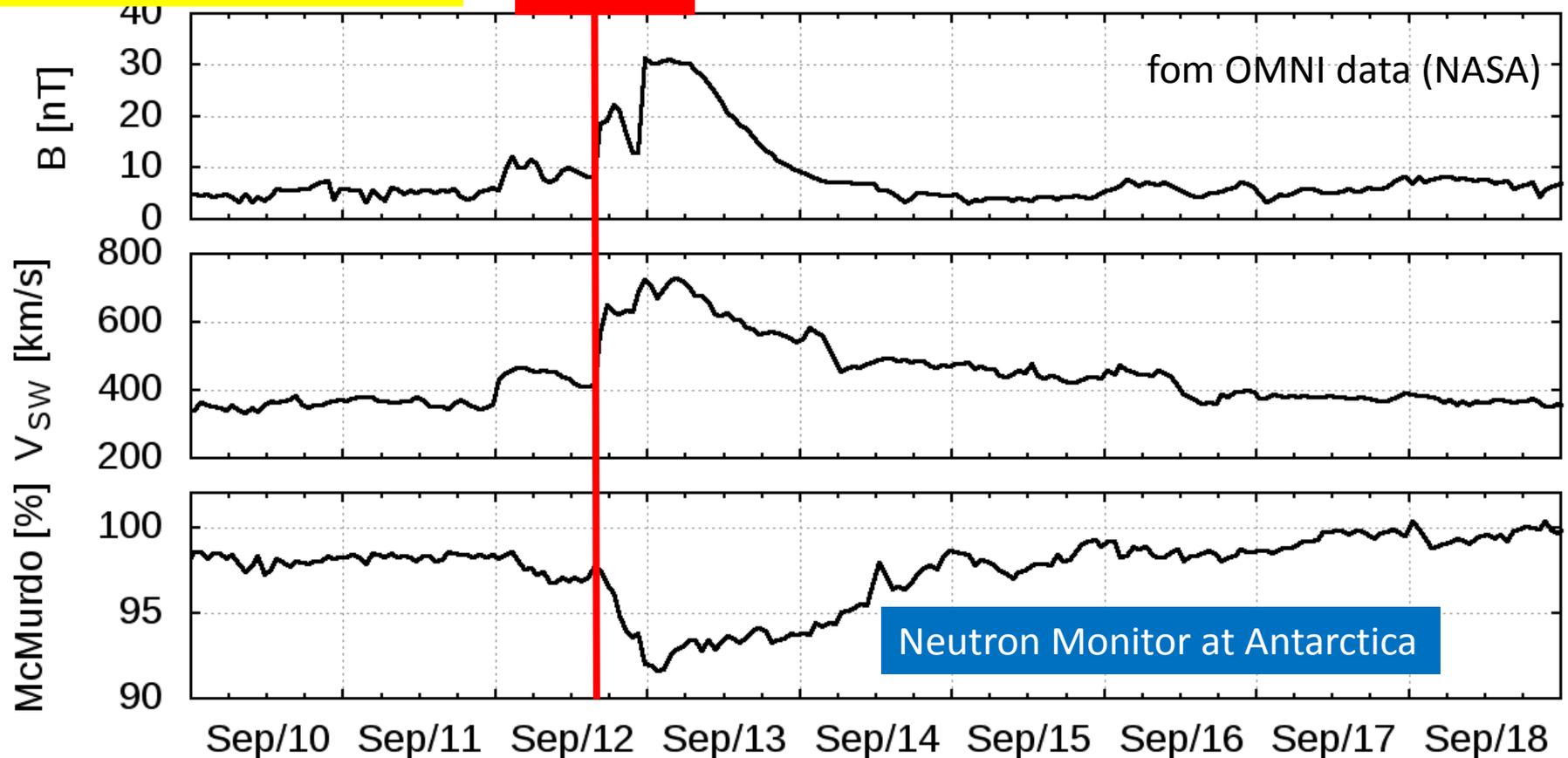P. Evenson[g], I. Sabbah[h] and M. Tokumaru[i]

[a]Shinshu University, [b]Chiba University, [c]CRS/INPE, [d]INPE, [e]Kuwait University, [f]University of Tasmania, [g]Bartol Research Institute, [h]PAAET, [i]STEL

Interplanetary Shock (IP-shock) and Galactic Cosmic Rays (GCRs)
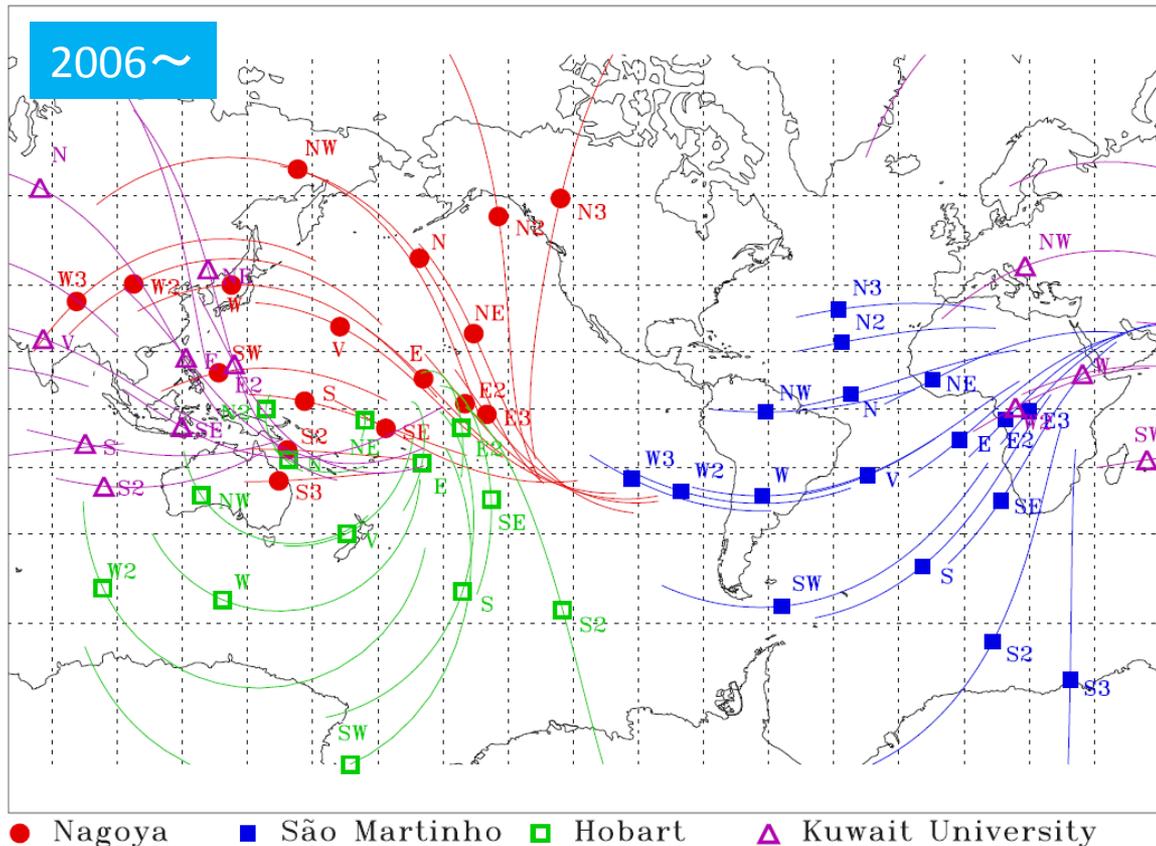

Sep/12, 2014 IP-shock event

IP-shock

fom OMNI data (NASA)

Neutron Monitor at Antarctica

Fast Solar Wind pushes ambient plasma ⇒ build an IP-Shock

Short term Decrease of GCR intensity : Forbush Decrease (Forbush, 1937)

⇒ GCR depleted region behind the IP-shock

Global Muon Detector Network（GMDN）

2006〜

Brazil

Kuwait

● Nagoya   ■ São Martinho   □ Hobart   △ Kuwait University

- Network of Four Muon Multi-Directional Detectors
- Directional Intensity of secondary cosmic rays
    → anisotropy of 〜60 GeV GCRs on an hourly basis
- Larmor radius 〜0.3 AU → Global Structure of interplanetary space
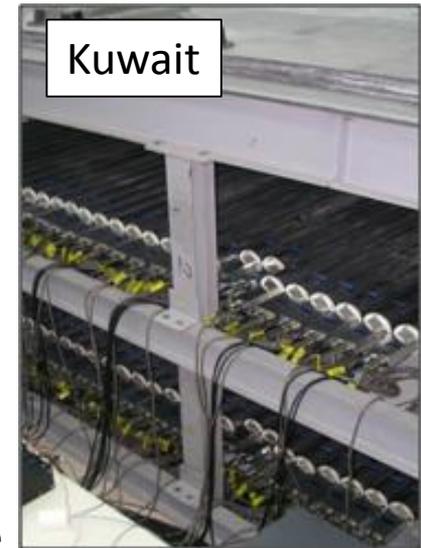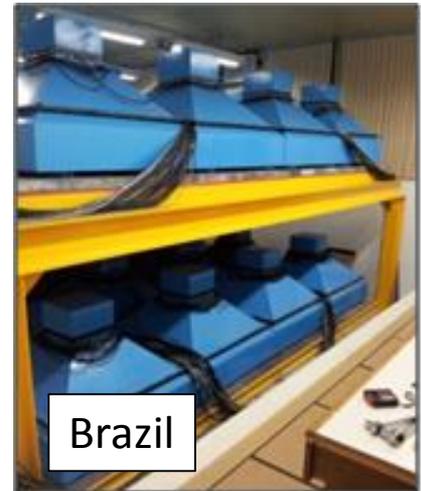
Advantages of the GMDN
High angular resolution, Wide angular range, reflecting Global structures

First Order Anisotropy and Spatial Density Gradient

Observed angular distribution $F(\mathbf{p})$ of GCRs $\Rightarrow$ the First Order Spherical Harmonics $F_1(\theta, \phi, p)$

$F_1(\theta, \phi, p) \propto \cos \chi (p)$
$\Rightarrow$ "Flow of cosmic rays" $\mathbf{S}(p)$

(Gleeson, 1969)

density U: High

Parker's transport equation

$\mathbf{S} = CU\mathbf{V}_{sw} - \mathbf{K} \cdot \dfrac{\partial U}{\partial \mathbf{r}}$

（Parker, 1965,
Gleeson & Axford, 1968）

$\left(\text{cf. Fick's law: } \mathbf{S} = -K\dfrac{\partial U}{\partial \mathbf{r}}\right)$
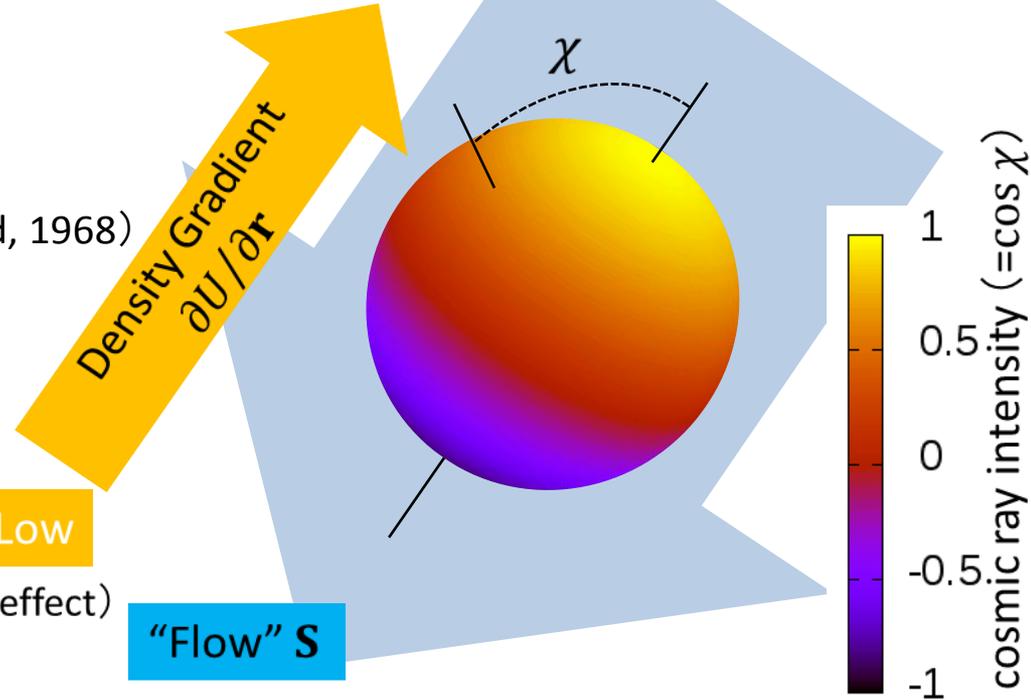
$U(p)$: cosmic ray density

$C = 1 - \dfrac{1}{3U}\dfrac{\partial(pU)}{\partial p}$

$\mathbf{V}_{sw}$: Solar wind velocity
$\mathbf{K}$: Diffusion tensor（diffusion coefficient + drift effect）

Density Gradient $\partial U/\partial \mathbf{r}$

χ

U: Low

"Flow" $\mathbf{S}$

cosmic ray intensity ($=\cos \chi$)

1

0.5

0

-0.5

-1

Corrections for Atmospheric (Murakami et al., 1979) and Geomagnetic (IGRF) effects
Best-Fitting of the Spherical Harmonics $\Rightarrow$ First Order Anisotropy
Solar wind velocity and Magnetic field（diff. tensor）in the OMNI data
                                        $\Rightarrow$ density gradient vector $\dfrac{1}{U}\dfrac{\partial U}{\partial \mathbf{r}}$ of GCRs
※assuming mean free path (m. f. p.) of GCRs based on Bieber et al., 1994 and 2004
parallel to the magnetic field: $\lambda_{||} = 7.2R_L$, perpendicular: $\lambda_\perp = 0.05\lambda_{||}$ ($R_L(t)$: Larmor radius @60 GeV)

1

Statistical analysis of IP-shock events -Superposed Epoch Analysis

1. Superposing temporal variations of density gradient at the timing of geomagnetic Storm Sudden Commencement (SSC, listed by GFZ)
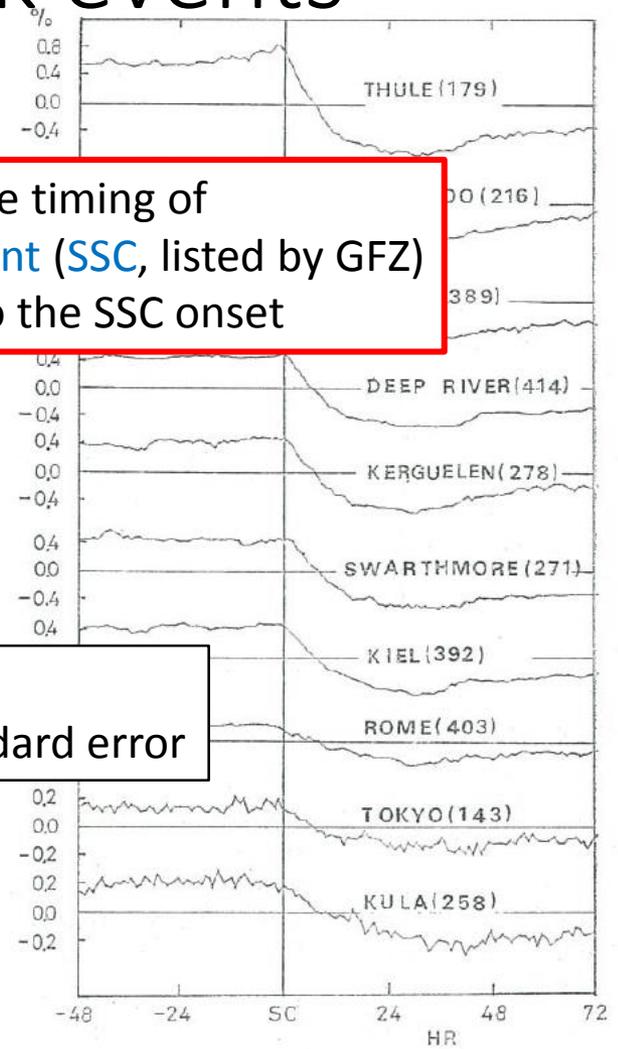2. Averaging the temporal variations at each relative time to the SSC onset

SSC: reference to IP-shock arrivals (Wang et al., 2006)

Example of superposed epoch analysis

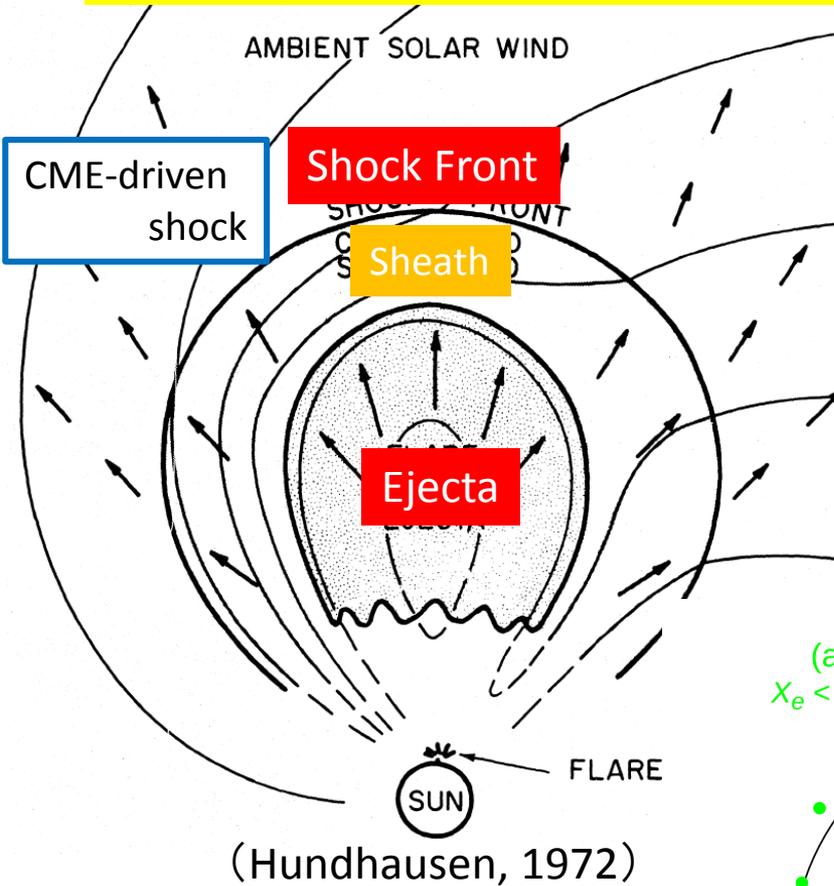Counting rate of Neutron Monitors at the polar region（～Scalar Density）   ※Not the density gradient
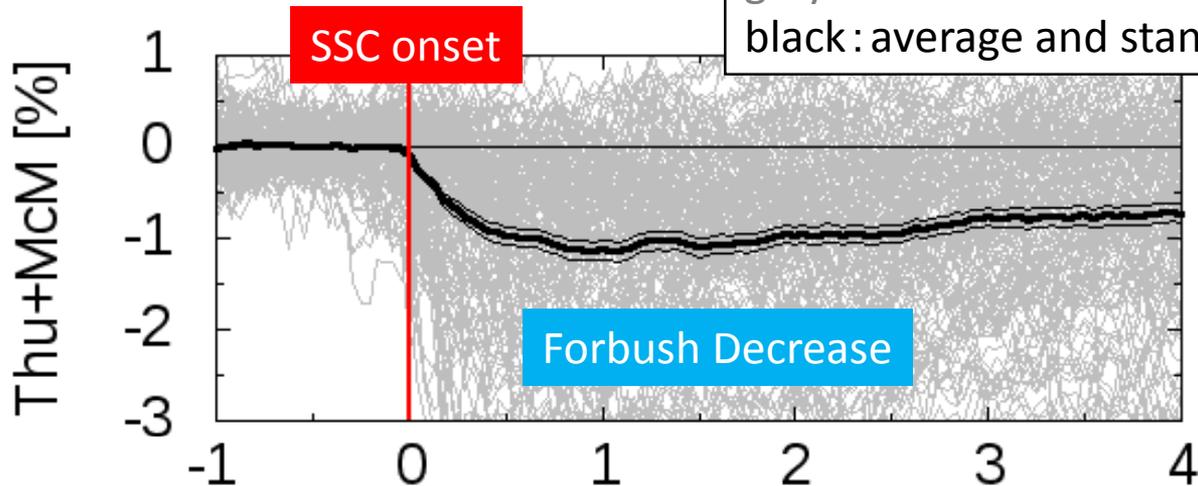
gray：each event
black：average and standard error

SSC onset

Forbush Decrease

Thu+McM [%]

Relative time to each SSC onset [day] (positive: after SSC)

THULE (179)

DO (216)

(389)

DEEP RIVER (414)

KERGUELEN (278)

SWARTHMORE (271)

KIEL (392)

ROME (403)

TOKYO (143)

KULA (258)

Wada & Suda, 1980

5

Extraction of CME (solar Coronal Mass Ejection) events

AMBIENT SOLAR WIND

CME-driven shock
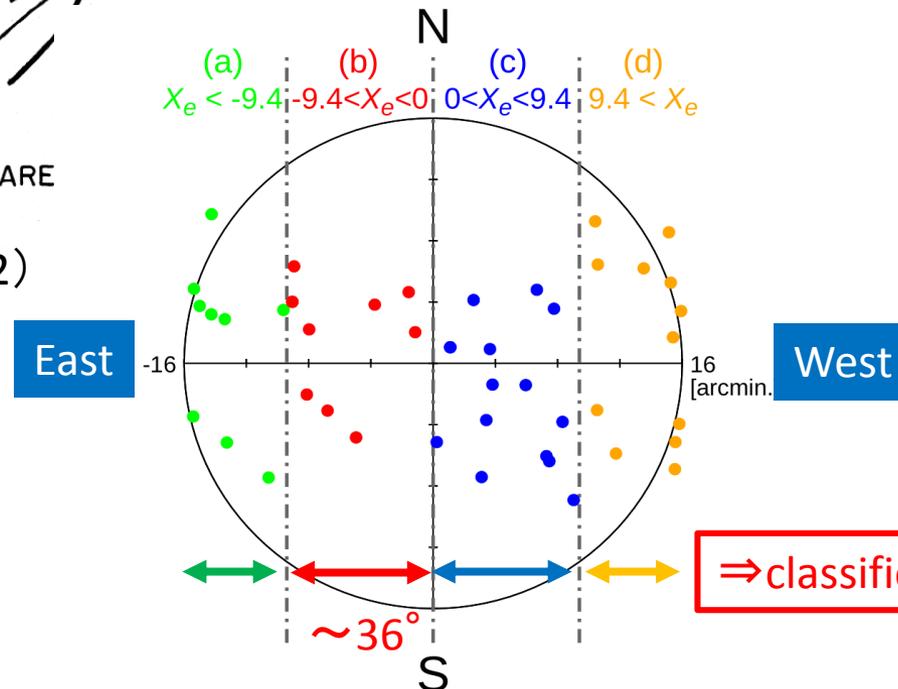
Shock Front

Sheath

Ejecta

FLARE

SUN

（Hundhausen, 1972）
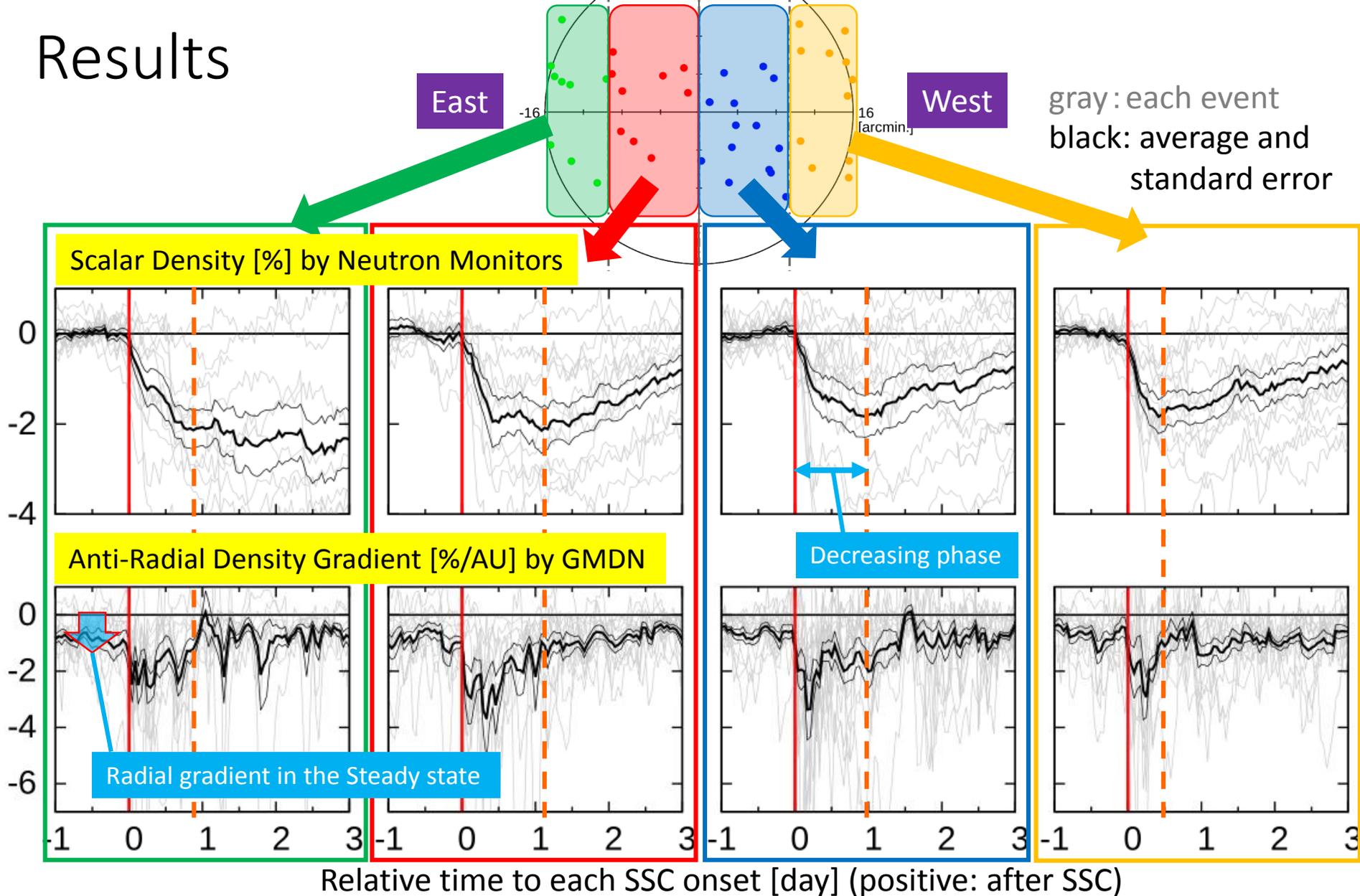
referring to the past Space Weather news (SW news)

The SW news is provided by NIT, Kagoshima College every day monitoring SDO, SOHO, ACE, and GOES satellite data, geomagnetic indices, and so on

Obtained 50 CME events in a period 2006-2014

Locations of the Eruptions on the sun-disk
（deduced from RHESSI flare list）

N
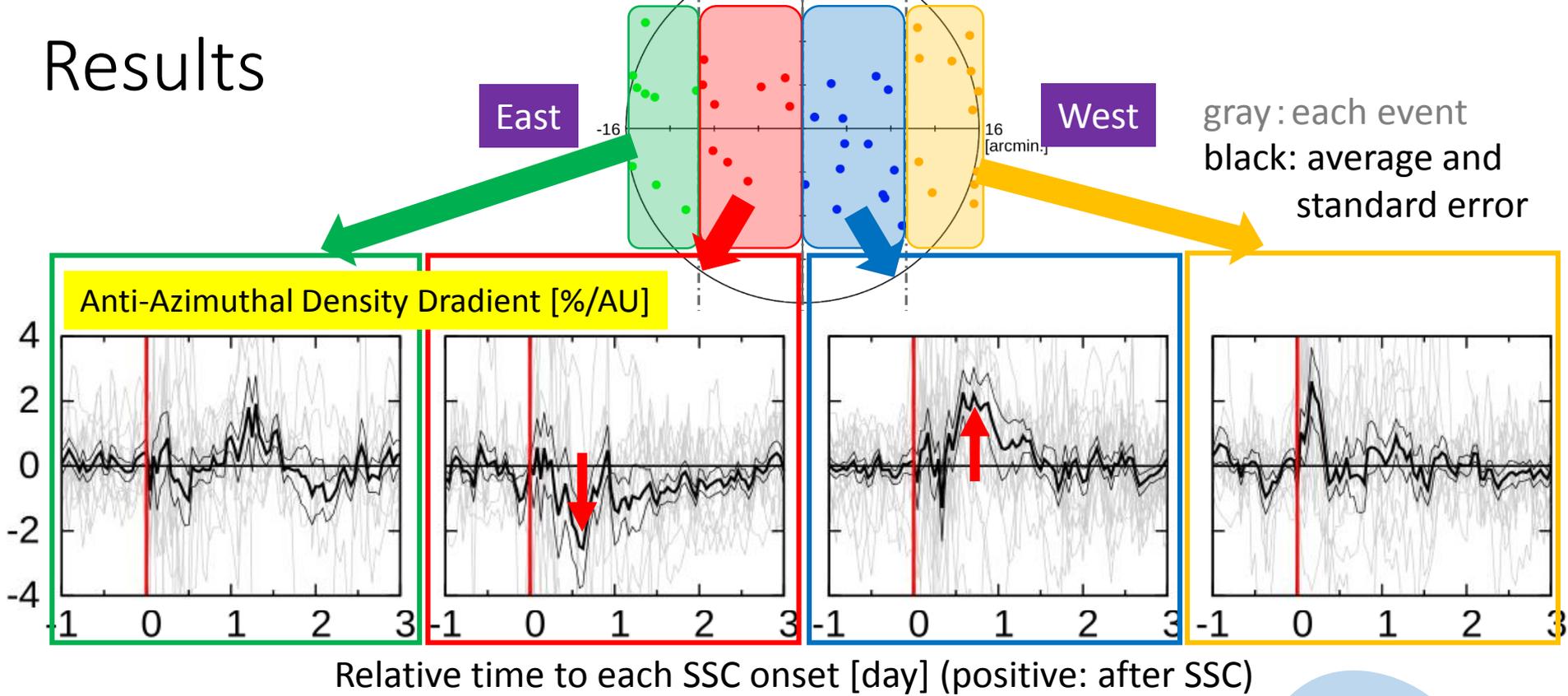
(a)   (b)   (c)   (d)
$X_e < -9.4$ $-9.4 < X_e < 0$ $0 < X_e < 9.4$ $9.4 < X_e$

East -16   16 [arcmin. West

~36°

S

⇒classified into 4 classes

6

Results

East West

gray : each event
black: average and
standard error

Scalar Density [%] by Neutron Monitors

Anti-Radial Density Gradient [%/AU] by GMDN

Decreasing phase

Radial gradient in the Steady state

Relative time to each SSC onset [day] (positive: after SSC)

Radial Density Gradient: $\frac{\partial U}{\partial r} = \frac{\partial t}{\partial r}\frac{\partial U}{\partial t} \approx -\frac{1}{V_{SW}}\frac{\partial U}{\partial t}$: Density Variation

Gradient of Western event: Pulsive enhancement ⇔ Eastern event: Slower enhancement

7

Results

East

West

gray : each event
black: average and
standard error

Anti-Azimuthal Density Dradient [%/AU]

Relative time to each SSC onset [day] (positive: after SSC)

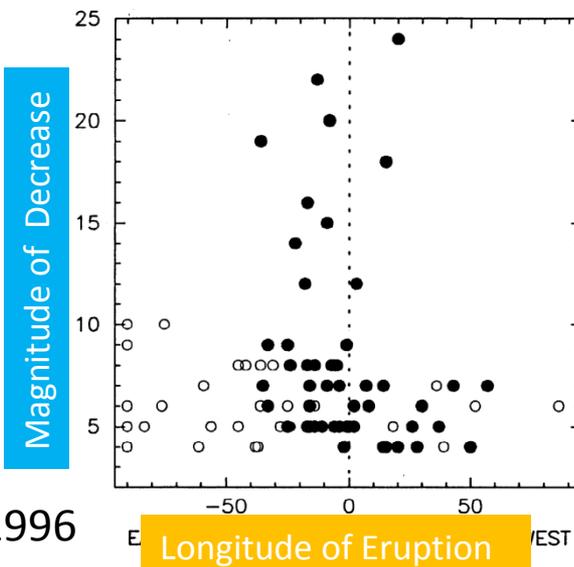Opposite directional enhancement ⇒
the Density Minimum around the Longitudinal Center

East eruption =
Earth encounters West flank of the shock

Slower enhancement of radial gradient in Eastern events
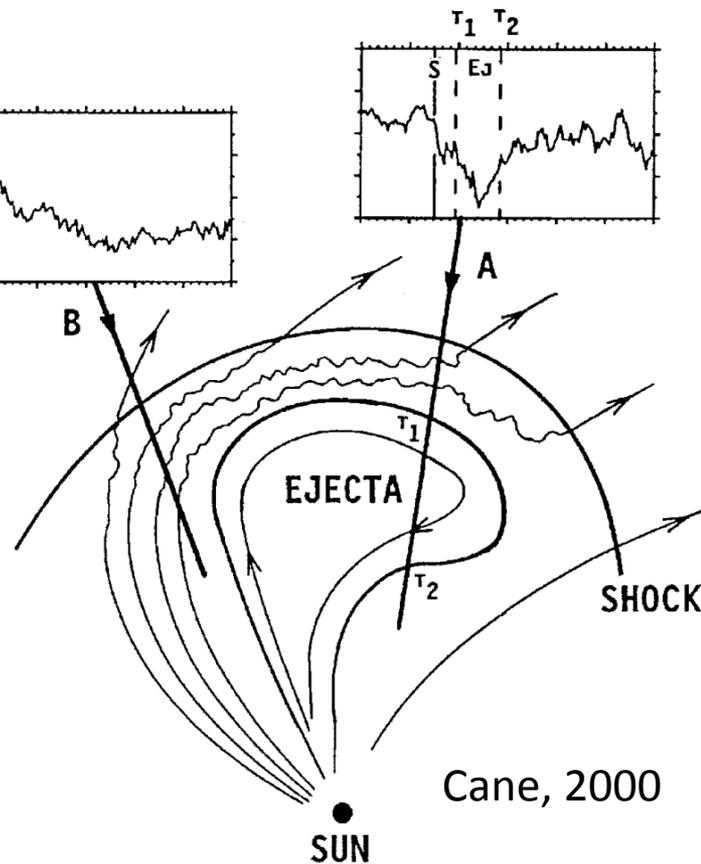⇒ Larger Spread of the depleted region in Western Side

GCR Depleted Region

East

West

Minimum

Density Gradient Vectors

Shock

8
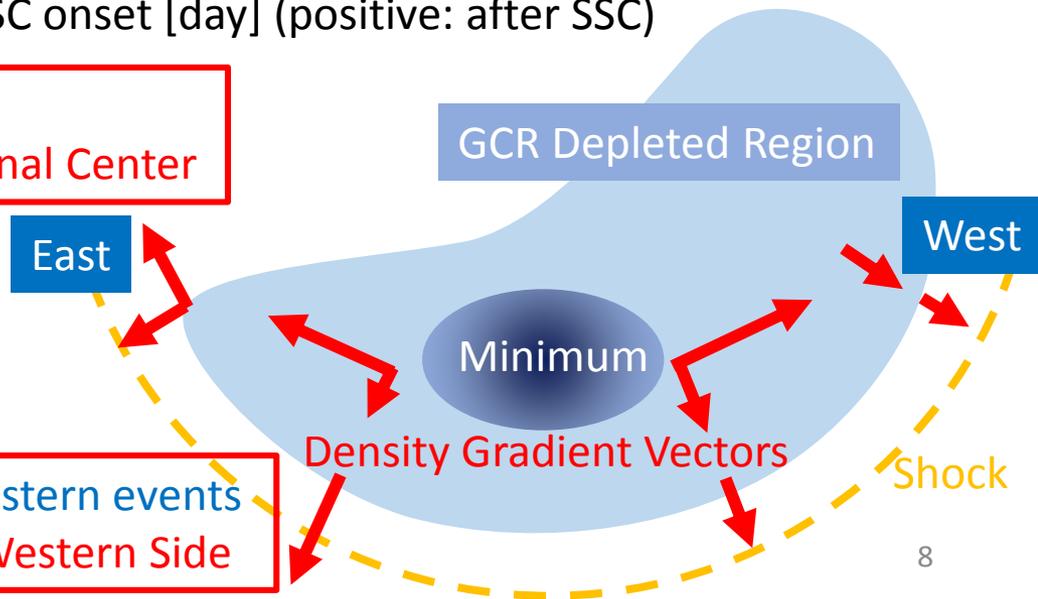
Discussions

Centered density Minimum
⇔ Centered Ejecta
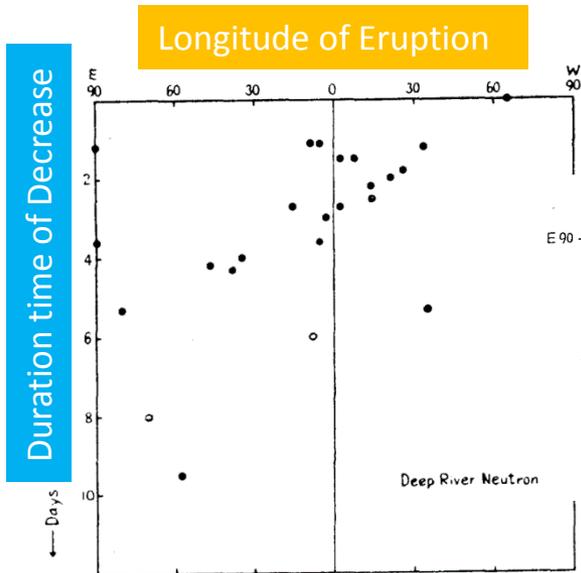
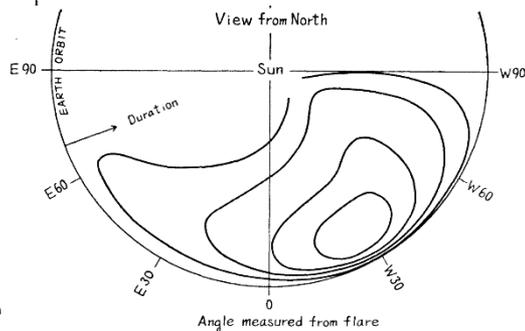Cane et al., 1996

Magnitude of Decrease

Longitude of Eruption

East-West asymmetry (larger spread in the western side)
⇔ Magnetic configuration of the Ambient Plasma
(arising from Parker's spiral field)

Longitude of Eruption

Duration time of Decrease

Sinno, 1962

Deep River Neutron

View from North

Cane, 2000

SUN

EJECTA

SHOCK

- Centered minimum = Ejecta effect
- East-West asymmetry = Shock effect

We confirmed these Average Features
using the Anisotropy observation
for the First time

9

END